

RESEARCH

Open Access



Combinatorial pathway enzyme engineering and host engineering overcomes pyruvate overflow and enhances overproduction of *N*-acetylglucosamine in *Bacillus subtilis*

Wenlong Ma^{1,2}, Yanfeng Liu^{1,2}, Xueqin Lv^{1,2}, Jianghua Li^{1,2}, Guocheng Du^{1,2} and Long Liu^{1,2*} 

Abstract

Background: Glucosamine-6-phosphate *N*-acetyltransferase (GNA1) is the key enzyme that causes overproduction of *N*-acetylglucosamine in *Bacillus subtilis*. Previously, we increased GlcNAc production by promoting the expression of GNA1 from *Caenorhabditis elegans* (CeGNA1) in an engineered *B. subtilis* strain BSGN12. In this strain overflow metabolism to by-products acetoin and acetate had been blocked by mutations, however pyruvate accumulated as an overflow metabolite. Although overexpression of CeGNA1 drove carbon flux from pyruvate to the GlcNAc synthesis pathway and decreased pyruvate accumulation, the residual pyruvate reduced the intracellular pH, resulting in inhibited CeGNA1 activity and limited GlcNAc production.

Results: In this study, we attempted to further overcome pyruvate overflow by enzyme engineering and host engineering for enhanced GlcNAc production. To this end, the key enzyme CeGNA1 was evolved through error-prone PCR under pyruvate stress to enhance its catalytic activity. Then, the urease from *Bacillus paralicheniformis* was expressed intracellularly to neutralize the intracellular pH, making it more robust in growth and more efficient in GlcNAc production. It was found that the activity of mutant CeGNA1 increased by 11.5% at pH 6.5–7.5, with the catalytic efficiency increasing by 27.5% to 1.25 s⁻¹ μM⁻¹. Modulated expression of urease increased the intracellular pH from 6.0 to 6.8. The final engineered strain BSGN13 overcame pyruvate overflow, produced 25.6 g/L GlcNAc with a yield of 0.43 g GlcNAc/g glucose in a shake flask fermentation and produced 82.5 g/L GlcNAc with a yield of 0.39 g GlcNAc/g glucose by fed-batch fermentation, which was 1.7- and 1.2-times, respectively, of the yield achieved previously.

Conclusions: This study highlights a strategy that combines pathway enzyme engineering and host engineering to resolve overflow metabolism in *B. subtilis* for the overproduction of GlcNAc. By means of modulated expression of urease reduced pyruvate burden, conferred bacterial survival fitness, and enhanced GlcNAc production, all of which improved our understanding of co-regulation of cell growth and metabolism to construct more efficient *B. subtilis* cell factories.

Keywords: *Bacillus subtilis*, *N*-Acetylglucosamine, Glucosamine-6-phosphate *N*-acetyltransferase, Pyruvate, Overflow, Urease

*Correspondence: longliu@jiangnan.edu.cn

¹ Key Laboratory of Carbohydrate Chemistry and Biotechnology, Ministry of Education, Jiangnan University, Wuxi 214122, China

Full list of author information is available at the end of the article



Background

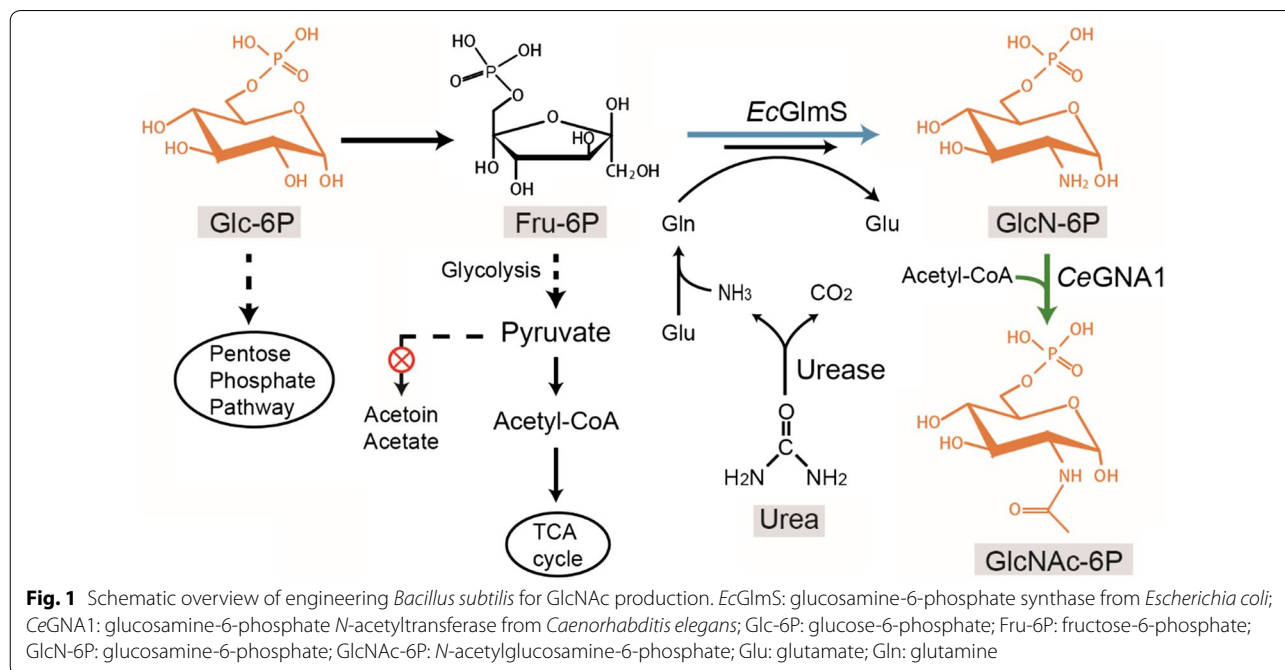
N-Acetylglucosamine (GlcNAc), a functional monosaccharide with many specific bioactivities, has received considerable attention for its commercial applications in the biomedical, food, and chemical industries [1, 2]. In the pathway toward biosynthesis of GlcNAc, glucosamine-6-phosphate *N*-acetyltransferase from *Caenorhabditis elegans* (*CeGNA1* [EC 2.3.1.4]), catalyzing the formation of GlcNAc-6-phosphate (GlcNAc-6P) by the acetylation of GlcN-6-phosphate (GlcN-6P) using the cofactor Ac-CoA, holds a key position (Fig. 1) [3, 4].

In previous studies, using 5'-terminus fusion engineering, we promoted heterogenous expression of *CeGNA1* and glutamine-fructose-6-phosphate aminotransferase from *Escherichia coli* (*EcGlmS*) in the recombinant *B. subtilis* strain BSGN12. Specifically, the expression level of *CeGNA1* was enhanced via fusing epitope tag cMyc to the 5'-terminus of *CeGNA1* gene and ribosome binding site (RBS) sequence engineering. Next, the expression level of *EcGlmS* was enhanced by fusing mRNA stabilizer Δ ermC+14/7 downstream of the strong P_{veg} promoter and inserting it in the *Bacillus subtilis* chromosome at the *als* locus. The enhanced expression of *CeGNA1* consumed AcCoA for GlcNAc-6-phosphate synthesis, which further facilitated pyruvate conversion to AcCoA and decreased pyruvate accumulation. The enhanced expression of *EcGlmS* consumed fructose-6-phosphate for GlcNAc-6-phosphate synthesis, competed with glycolysis and decreased pyruvate formation. Also, the enhanced expression of *CeGNA1* and *EcGlmS* decreased pyruvate

accumulation and promoted GlcNAc production in the recombinant *B. subtilis* strain BSGN12. However, the fact that overflow of metabolic by-products acetoin and acetate had been blocked by mutations in *alsRSD* and *ackA*, meant that pyruvate accumulated as an overflow metabolite in this strain (Fig. 1) [5, 6].

Though overexpression of *CeGNA1* and *EcGlmS* decreased pyruvate accumulation for GlcNAc-6P synthesis, there was still a small amount of pyruvate (~3.5 g/L) that accumulated in the broth during fermentation. Herein, we found that the residual pyruvate acidified the extracellular pH (pH_{ex}) and intracellular pH (pH_{in}), with the lowest pH_{ex} and pH_{in} being 5.7 and 6.0 for BSGN12 during fermentation. The pH_{in} critically affects bacterial cell physiology, such as protein synthesis and enzyme activity [7–10]. The activity of *CeGNA1* is pH-dependent with an optimum pH of 8.2, which is similar to other GNA1 homologues that generally function in alkaline conditions (pH 7.4–9.7), thus it is crucial to maintain intracellular pH homeostasis for the enhanced activity of *CeGNA1* and improved production of GlcNAc [4].

In this study, for increasing GlcNAc production, error-prone PCR (Ep-PCR) based directed evolution of *CeGNA1* was conducted during pyruvate stress to enhance its catalytic activity, and one mutant *CeGNA1*-Q155V/C158G, whose activity in the pH 6.5–7.5 increased by 11.5% with the catalytic efficiency increasing by 27.5% to $1.25 \text{ s}^{-1} \mu\text{M}^{-1}$, was obtained. Shake flask fermentation showed that the evolved *CeGNA1*-Q155V/C158G increased the GlcNAc titer by 11.3%



to 20.6 g/L. Next, the urease from *Bacillus paralicheniformis* was expressed under the control of exponential phase-dependent promoter (P_{hag}) to neutralize the pH_{in} . Expression of urease enhanced urea utilization and increased the pH_{in} from 6.0 to 6.8, making it more robust in growth and more efficient in GlcNAc production, with the GlcNAc titer and yield reaching 25.6 g/L and 0.43 g GlcNAc/g glucose, respectively. In a 3-L fermenter, the final strain overcame pyruvate overflow and produced 82.5 g/L GlcNAc with a yield of 0.39 g GlcNAc/g glucose, which was 1.7- and 1.2-times that of the control. The data highlight the importance of pathway enzyme engineering and host engineering in regulating activities of key enzyme *CeGNA1* to overcome pyruvate overflow and efficiently produce GlcNAc in engineered *B. subtilis* factories.

Materials and methods

Strains, plasmids, and culture conditions

The bacterial strains and plasmids used in this study are listed in Table 1. The primers are listed in the

Additional file 1: Table S1. BSGN12 ($\Delta nagP\Delta gamP\Delta gamA\Delta nagA\Delta nagB\Delta ldh\Delta pta\Delta ackA::lox72$, $\Delta alsRSD::Pveg-\Delta ermC+14/7A-ecgIm$), which secreted pyruvate into the medium during fermentation, was used as the host strain [6]. During the construction of the strains and plasmids, all strains were grown at 37 °C in standard Luria–Bertani broth (LB) (10 g/L tryptone, 5 g/L yeast extract, 10 g/L NaCl) or LB agar plates, with an appropriate concentration of antibiotics used for selection (100 µg/mL ampicillin, 25 µg/mL kanamycin, or 30 µg/mL zeocin).

During shake flask and fed-batch fermentations, the following fermentation medium was used: urea, 5 g/L; $(NH_4)_2SO_4$ 6 g/L; yeast extract, 12 g/L; tryptone, 6 g/L; $K_2HPO_4 \cdot 3H_2O$, 18.75 g/L; $MgSO_4$, 3 g/L; $FeSO_4 \cdot 7H_2O$, 0.06 g/L; $CaCl_2$, 0.06 g/L; and $NiCl_2 \cdot 6H_2O$, 0.12 g/L. Glucose was sterilized separately, and added to the shake flask to a final concentration of 60 g/L. Xylose (final concentration, 10 g/L) was added to the fermentation medium when the optical density at 600 nm (OD_{600}) reached 0.6 to induce the expression of urease controlled by P_{xyIA} promoter.

Table 1 Strains and plasmids used in this study

	Characteristics	References
<i>Strains</i>		
BSGN5	<i>B. subtilis</i> 168 derivate, $\Delta nagP\Delta gamP\Delta gamA\Delta nagA\Delta nagB\Delta ldh::lox72$	[30]
BSGN10	<i>B. subtilis</i> 168 derivate, $\Delta nagP\Delta gamP\Delta gamA\Delta nagA\Delta nagB\Delta ldh\Delta alsRSD::lox72$	[5]
BSGN12	<i>B. subtilis</i> 168 derivate, $\Delta nagP\Delta gamP\Delta gamA\Delta nagA\Delta nagB\Delta ldh\Delta pta\Delta ackA::lox72$, $\Delta alsRSD::Pveg-\Delta ermC+14/7A-ecgImS$	[6]
BSGN12- P_{veg} -urease	BSGN12 derivate, expression of urease from <i>Bacillus paralicheniformis</i> under the control of promoter P_{veg}	This study
BSGN12- P_{xyIA} -urease	BSGN12 derivate, expression of urease from <i>Bacillus paralicheniformis</i> under the control of promoter P_{xyIA}	This study
BSGN12- P_{abrB} -urease	BSGN12 derivate, expression of urease from <i>Bacillus paralicheniformis</i> under the control of promoter P_{abrB}	This study
BSGN13	BSGN12 derivate, expression of urease from <i>Bacillus paralicheniformis</i> under the control of promoter P_{hag}	This study
BSGN12- P_{ffh} -urease	BSGN12 derivate, expression of urease from <i>Bacillus paralicheniformis</i> under the control of promoter P_{ffh}	This study
BSGN12- P_{licH} -urease	BSGN12 derivate, expression of urease from <i>Bacillus paralicheniformis</i> under the control of promoter P_{licH}	This study
<i>Plasmids</i>		
pZ6	pMD18-T containing <i>lox71-zeo-lox66</i> cassette	[19]
pTSC	Em ^r Amp ^r ; temperature sensitive in <i>B. subtilis</i>	[19]
pP ₄₃ -cMyc (M-Rm)- <i>CeGNA1</i>	key enzyme <i>CeGNA1</i> expressing vector	[6]
pP ₄₃ -cMyc (M-Rm)- <i>CeGNA1</i> -Q155V/C158G	pP ₄₃ -cMyc (M-Rm)- <i>CeGNA1</i> derivate, with 155Gln and 158Cys of <i>CeGNA1</i> mutated to 155Val and 158Gly, respectively	This study
pP ₄₃ -6His- <i>CeGNA1</i>	pP ₄₃ NMK derivate with <i>CeGNA1</i> cloned	[6]
pCold- <i>CeGNA1</i>	pCold III derivate, containing wild type <i>CeGNA1</i> , with His tag fused to the N terminal	This study
pCold- <i>CeGNA1</i> -Q155V/C158G	pCold III derivate, containing mutant <i>CeGNA1</i> -Q155V/C158G, with His tag fused to the N terminal	This study
pP _{veg} - <i>EcGImS</i> -1	pUC57-Amp derivate, containing the synthesized expression cassette, terminator I- P_{veg} -TSS-RBS ₀ -terminator II	[6]
pStop1622	Amp ^r , Tet ^r , <i>E. coli</i> - <i>B. megaterium</i> shuttle vector	[31]

Detection of pH_{in}

The pH_{in} of cells were assayed using a pH-sensitive fluorescent probe 2',7'-bis-(2-carboxyethyl)-5-(and 6-)-carboxyfluorescein succinimidyl ester (BCECF-AM) (Beyotime Institute of Biotechnology, China) [11]. Firstly, cells during different periods were harvested by centrifugation at 14,972g for 10 min. Then the cell pellets were resuspended in PBS buffer (50 mM K₂HPO₄, 50 mM KH₂PO₄, pH 7.0), washed twice and diluted to an OD₆₀₀ of 3.0. Secondly, 400 μL of the above bacterial suspension and 4 μL valinomycin were added to brown tubes and incubated at 30 °C for 30 min. Thirdly, 1 μL of BCECF-AM was added into the brown tubes and incubated at 30 °C for 20 min; then 200 μL of the reaction solution was taken out and centrifuged at 14,972g for 5 min. Lastly, 150 μL of the reaction solution and the supernatant were taken out to measure the fluorescence intensity. Measurements of the fluorescence intensity were performed using a Cytation 3 imaging reader system (BioTek, Winooski, VT, USA). The excitation wavelengths were 490 and 440 nm. The emission wavelength was 525 nm. The relative fluorescence intensity (RFI) was calculated as follows: $RFI = [(I_{490})_{total} - (I_{490})_{supernate}] / [(I_{440})_{total} - (I_{440})_{supernate}]$. Based on the values of lg (RFI), the intracellular pH was calculated from the standard curve. Measurements were performed with three biological replicates.

Random mutagenesis of CeGNA1 with Ep-PCR

Ep-PCR was performed using a GeneMorph II Random Mutagenesis Kit (Agilent Technologies, Santa Clara, CA, USA). Mutagenic amplifications were conducted by two separate processes to optimize the quantities of template (0.1, 1, 10, or 100 ng) and the number of amplification cycles (15, 20, 25, and 30). After process optimization, we found that 1 ng of template and 20 cycles of amplification were suitable for the production of one or two amino acids containing mutants. After the amplification under the suitable conditions using the primer pair er-ceN-F1/er-ceN-R1, the PCR products were purified and ligated with the linearized plasmid pP43-cMyc (M-Rm)-CeGNA1 [6], which had been PCR amplified using the primer pair er-ceN-F2/er-ceN-R2 to remove the wild type *cegna1* gene. The ClonExpress™ II kit (Vazyme Biotech Co., Ltd) was used for the ligation, and then the ligation products were used to transform *Escherichia coli* JM109 cells. The resulting colonies growing on the plates were washed down with sterile water, inoculated into LB liquid medium and then cultured for 8 h before plasmid DNA were extracted. Then, the plasmid DNA were transformed into the engineered host strain BSGN12. Preliminary screening of high-yield mutants was conducted in a

96-well plate, using the Reissig method [12]. Finally, the high-yield mutants were confirmed for shake flask fermentation. The mutagenesis selection process is shown in Additional file 1: Fig. S1.

Purification and activities determination of CeGNA1 and its mutant

For the purification of CeGNA1, the wild type *cegna1* gene was amplified from the plasmid pP₄₃-6His-CeGNA1 using the primer pair HisCeN-F/HisCeN-R, and then ligated with the expression plasmid pCold III (linearized by PCR amplification with the primer pair pCold-F/pCold-R) using the ClonExpress™ II kit (Vazyme Biotech Co., Ltd), yielding pCold-CeGNA1. Then pCold-CeGNA1 was used as the template to generate pCold-CeGNA1-Q155V/C158G using the one-step site-directed plasmid insertion protocol [13]. The primers used were Q155V/C158G-F and Q155V/C158G-R.

Strains expressing of pCold-CeGNA1 or pCold-CeGNA1-Q155V/C158G were cultured in LB medium, and protein expression was induced by the addition of 1 mM isopropyl-β-D-thiogalactopyranoside (IPTG) following a temperature downshift from 37 to 15 °C. After cultivation for 24 h following induction, the strains were harvested by centrifugation at 6000×g for 10 min, lysed by sonication on ice, resuspended in 50 mM Tris-HCl buffer (pH 7.5), and then purified via nickel affinity using a Ni²⁺ column [14]. The eluted His₆-tagged protein was dialyzed against 50 mM Tris/HCl (pH 7.5) and 5.0 mM MgCl₂, and its purity was confirmed by sodium dodecyl sulfate polyacrylamide gel electrophoresis (SDS-PAGE). The SDS-PAGE was performed as described in Additional file 1: Fig. S3. No denaturants were added before the SDS-PAGE. The reductant dithiothreitol (DTT) added was 30 μM. The protein concentration was determined using the Bradford assay with BSA as standard.

CeGNA1 activity was determined using the 5,5'-dithiobis (2-nitrobenzoic acid) (DTNB) method by measuring the amount of free thiol groups generated during acetyl transfer in Tris-HCl buffer (pH 7.5, 50 mM) [4]. A control without the addition of enzyme was used. The amount of CoASH produced was calculated based on $E = \epsilon l c$ with $\epsilon^{DTNB} = 137,000 \text{ M}^{-1} \text{ cm}^{-1}$ and $l = 1 \text{ cm}$. One unit of GNA1 activity was defined as the amount of enzyme that produced 1 nmol of CoASH per minute under the analysis condition. To determine pH stability of CeGNA1, the wild-type and mutant enzymes were incubated in Tris-HCl buffer (pH 5.5 to 7.5, 50 mM) at 30 °C for 12 h. Then the CeGNA1 activity was measured at pH 7.5. For kinetics, 50 ng of enzyme was used, and the GlcN-6P concentrations were 50, 100, 150, 200, 500, 1000, and 2000 μM.

Expression of urease from *Bacillus paralicheniformis*

The urease gene cluster was integrated at *yoqM* loci, which is a nonessential gene in *B. subtilis* according to SubtiWiki (<http://subtiwiki.uni-goettingen.de/>), and inactivation of it could improve the yield and purities of poly-histidine tagged protein produced in *B. subtilis* according to the US patent WO2016050680A1 [15]. The urease gene cluster *ureABCEFGDH* was amplified from the genomic DNA of *B. paralicheniformis* using the primer pairs ure-F(Pveg)/ure-R, ure-F(PxylA)/ure-R or ure-F(PabrB)/ure-R, respectively [16]. The promoters P_{veg} , P_{xylA} , P_{abrB} , P_{hag} , P_{ffh} , and P_{licH} were amplified from the plasmid pP_{veg}-*EcGlmS*-1, pStop1622, and the genomic DNA of *B. subtilis* 168, respectively [17]. Then, the front and back homology arms, amplified from the genomic DNA of *B. subtilis* 168, and the zeocin resistance gene, amplified from the plasmid p7Z6, were fused with the corresponding promoters and urease coding genes in the order of *yoqM* (L)-zeo-promoter-*ureABCEFGDH*-*yoqM* (R) using overlap extension PCR [18]. Finally, integration of the fusion products into the chromosome of BSGN12 was conducted as described before [19]. The primer pairs ure 1-F/ure 1-R and ure 2-F/ure 2-R were used in colony PCR for selecting the correct mutants.

Fed-batch fermentation in a 3-L bioreactor

Fed-batch fermentation of BSGN13, transformed with the plasmid pP₄₃-cMyc (M-Rm)-*CeGNA1*-Q155V/C158G, was performed in a 3-L fermenter (BioFlo115, New Brunswick Scientific Co., Edison, NJ, USA). Ninety milliliters of seed culture that were cultured in 500-mL flasks for 8–10 h was added to the 3-L fermenter with an initial 1.7 L of fermentation medium. The pH was maintained at 7.3 automatically via the addition of ammonium hydroxide (50% [vol/vol]), and the temperature was maintained at 37 °C. The aeration and agitation rates were 1.5 vvm and 800 rpm, respectively. The initial glucose concentration was 40 g/L, and during fermentation it was maintained at 2–10 g/L using an automatic glucose analyzer.

Analytical methods

The concentration of urea in the fermentation medium was quantified by high-pressure liquid chromatography with fluorescence detection after automated derivatization with xanthydro [20]. The concentration of glucose, GlcNAc, and pyruvate in the fermentation broth was analyzed by HPLC as described before [6]. Cell growth was monitored by measuring the absorbance at 600 nm (OD₆₀₀). The correlation between OD₆₀₀ and dry cell weight (DCW) was OD₆₀₀ of 1 = 0.35 DCW (g/L) [21].

All the experiments were performed independently at least three times.

Results

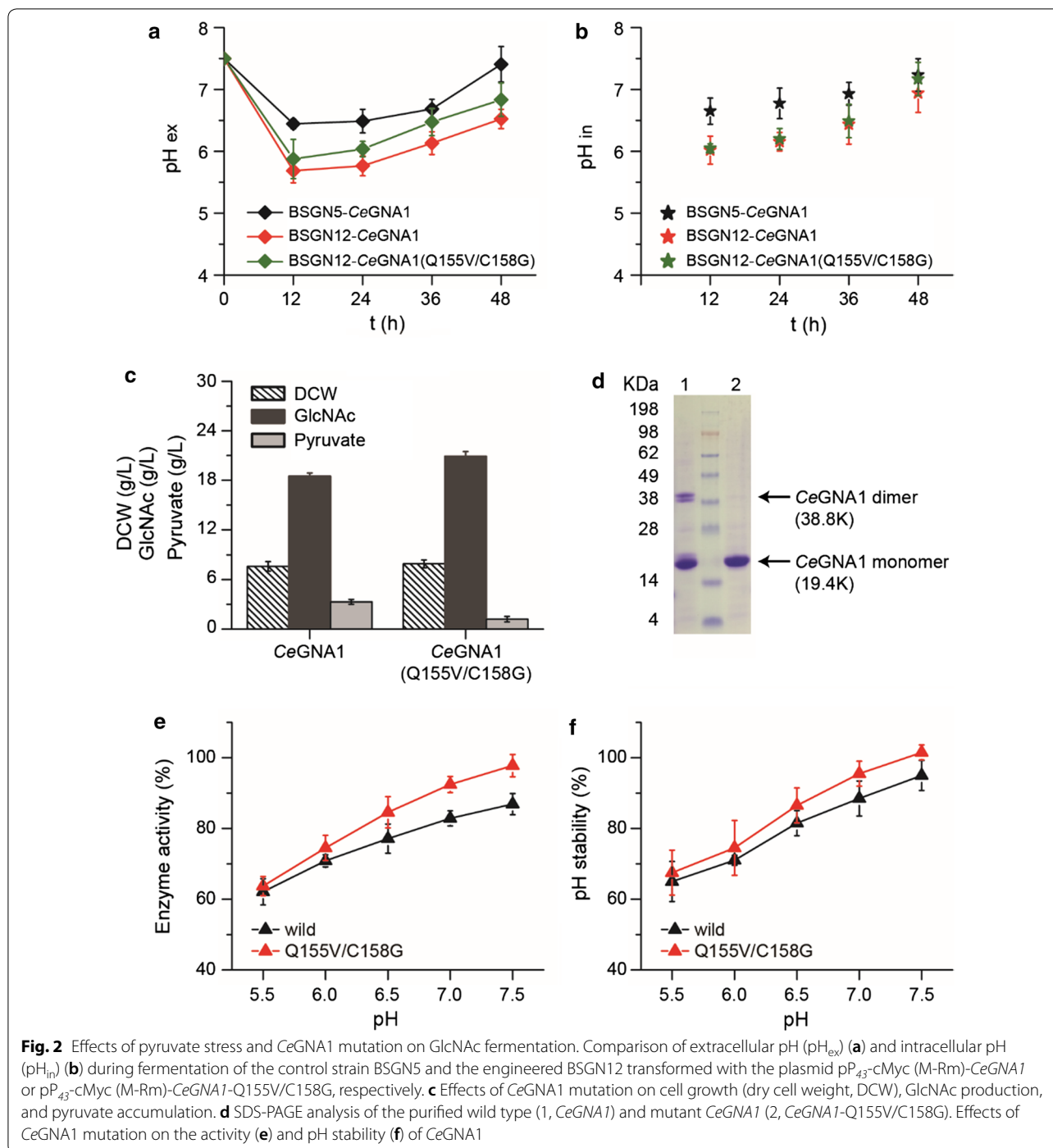
Pyruvate stress decreased pH_{ex} and pH_{in}

During fermentation of BSGN12, transformed with the plasmid pP₄₃-cMyc (M-Rm)-*CeGNA1*, pyruvate was produced as an overflow metabolite and lowered the pH_{ex} from the initial 7.5 to around 5.7, which was 0.8 units lower than 6.5 as was observed in strain BSGN5 (Fig. 2a). To confirm the lowering of pH_{in} caused by the pyruvate stress, the pH_{in} of BSGN12 cells was measured using a pH-sensitive fluorescent probe BCECF-AM and found that the pH_{in} varied from 6.0 to 6.9 depending on the cellular state, which was decreased compared to that of strain BSGN5 (ranging from 6.6 to 7.2) (Fig. 2b). Because *CeGNA1* has optimum activity in alkaline conditions (pH 7.4–9.7), it was assumed that the decreased pH_{in} caused a decrease of *CeGNA1* catalytic efficiency, which limited GlcNAc production.

Mutations of *CeGNA1* enhanced its activity and promoted GlcNAc production

To improve the catalytic efficiency of enzyme *CeGNA1* under pyruvate stress, a library of *CeGNA1* mutants with an average mutation rate of one or two amino acid changes per protein was generated using Ep-PCR. After screening approximately 10⁴ Ep-PCR clones, 15 mutants with enhanced GlcNAc titer were selected and retested in batch cultures and one evolved mutant, *CeGNA1*-Q155V/C158G, which increased the GlcNAc titer from 18.5 to 20.9 g/L and decreased the extracellular pyruvate from 3.5 to 1.2 g/L, was identified and further characterized (Fig. 2c). The mutagenesis selection process is shown in Additional file 1: Fig. S1. During fermentation of BSGN12, transformed with the mutant *CeGNA1*-Q155V/C158G, the lowest pH_{ex} increased to 5.9, which was slightly higher than that before (5.7) (Fig. 2a). Specific activity analysis of *CeGNA1* in the lysis supernatant found that it increased by 21.7% to 1060 U/mg [6]. However, the decreased pyruvate concentration had little impact on pH_{in} (Fig. 2b). This increase of pH_{ex} and GlcNAc titer might be due to the enhanced catalytic efficiency of *CeGNA1*-Q155V/C158G during acidic stress.

To gain further insight into the effects of Q155V/C158G mutations on catalytic efficiency, the mutant enzyme *CeGNA1*-Q155V/C158G was expressed using an *E. coli* expression system, purified, and verified by SDS-PAGE, and its activity in acidic pH was measured. As shown in Fig. 2d, this size was consistent with the calculated protein mass of 19.4 kDa. Compared with the wild-type *CeGNA1*, the mutant *CeGNA1*-Q155V/C158G lacked the 38.8 kDa band representing a homodimer,



which was probably due to the C158G mutation resulting in the lack of a disulfide bond formed between the two monomers, thereby reducing the thermostability of the homodimer such that *CeGNA1*-Q155V/C158G can completely denature in the same conditions when preparing SDS-PAGE [4]. Analysis of the activity and pH stability of mutant *CeGNA1*-Q155V/C158G showed that

it increased with the increasing pH and was higher than that of the wild type (Fig. 2e, f). Especially in pH 6.5–7.5, the activity of the mutant protein was 11.5% higher than that of the wild type. Kinetic data analysis showed that the Michaelis constant (K_m value) of *CeGNA1*-Q155V/C158G for GlcN-6-P (122 μ M) was 12.2% lower than that of the wild type, and the k_{cat}/K_m of *CeGNA1*-Q155V/

Table 2 Kinetic data of wild-type and Q155V/C158G CeGNA1 for GlcN-6-P

	K_m (μM)	k_{cat} (s^{-1})	k_{cat}/K_m ($\text{s}^{-1} \mu\text{M}^{-1}$)
CeGNA1	139 ± 9	136 ± 1.1	0.98
CeGNA1-Q155V/C158G	122 ± 6	151 ± 1.5	1.23

C158G ($1.25 \text{ s}^{-1} \mu\text{M}^{-1}$) was 27.5% higher than that of CeGNA1 ($0.98 \text{ s}^{-1} \mu\text{M}^{-1}$) (Table 2). These results indicated that the mutations Q155V/C158G increased the substrate-binding ability and improved its catalytic efficiency.

Previous studies revealed that formation of two disulfide bonds, one formed between Cys158 from the A and B chains and another between the conserved Cys141 and CoA, inhibited the enzyme activity [4]. The increased activity of mutant CeGNA1-Q155V/C158G might be due to the replacement of Cys158 by Gly158 preventing the formation of the disulfide bonds and relieving the inhibition of enzyme CeGNA1 by CoA. Comparison of the GlcNAc titer in strains expressing CeGNA1 with single Q155V or C158G mutations demonstrated that the single mutation of 155Q to 155V had little effect on GlcNAc production, and the single mutation of 158C to 158G was sufficient for the improved yield of GlcNAc (Additional file 1: Fig. S2). Therefore, it could be speculated that 158Cys was the main factor affecting GlcNAc production. Further saturation mutation of C158 site showed that most of the mutants increased GlcNAc production compared with the wild CeGNA1, and confirmed the conclusion that mutation of Gly158 prevents the formation of the disulfide bonds and relieves the inhibition of enzyme CeGNA1 by CoA (Additional file 1: Fig. S2).

Expression of urease increased the pH_{in} and promoted GlcNAc production

To generate urease-expressing strains, two urease expression cassettes containing the *ureABCEFGDH* gene cluster from *B. paralicheniformis*, one under the control of constitutive promoter P_{veg} and the other under the xylose inducible promoter P_{xyLA} , were integrated into the *yoqM* loci, resulting in BSGN12- P_{veg} -urease and BSGN12- P_{xyLA} -urease, respectively (Fig. 3a). Shake flask fermentation of BSGN12- P_{veg} -urease and BSGN12- P_{xyLA} -urease with the plasmid pP43-cMyc (M-Rm)-CeGNA1-Q155V/C158G were conducted in the fermentation medium with 5.0 g/L urea. Expression of urease under the control of promoters P_{veg} and P_{xyLA} strongly promoted urea utilization, with 4.3 g/L urea being consumed during the first 12 h

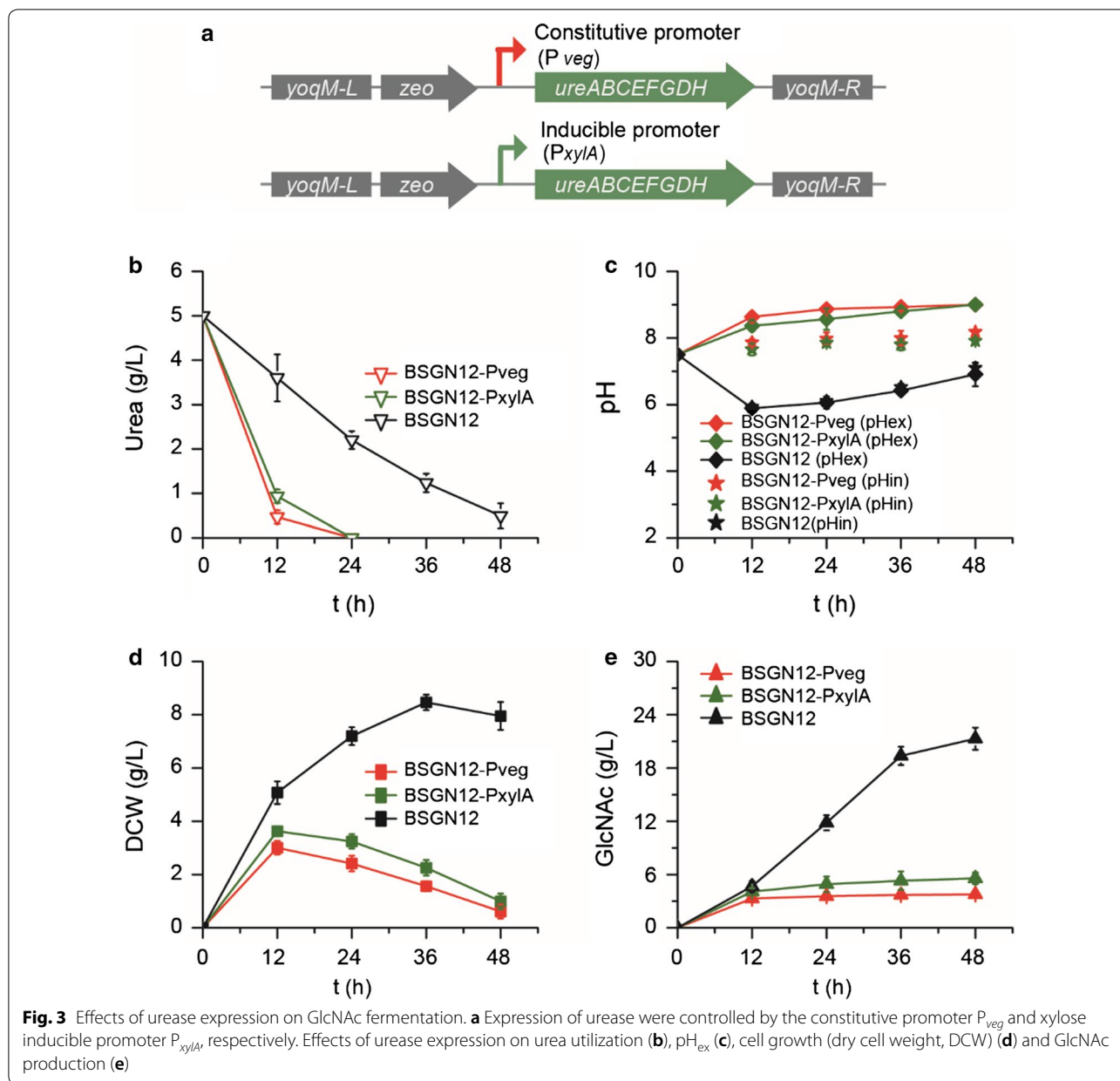
(Fig. 3b). In contrast, urea utilization in the starting strain BSGN12 was slow, with 1.4 g/L urea being consumed during the first 12 h, and a total of 3.6 g/L urea consumed within 48 h. This rapid utilization of urea in BSGN12- P_{veg} -urease and BSGN12- P_{xyLA} -urease alkalized the culture to a pH of roughly 8.5 (Fig. 3c). Because urease was expressed intracellularly, alkalization of pH_{ex} indicated alkalization of pH_{in} (rising to 7.9), and this limited cell growth as well as GlcNAc production, with the maximum DCW reaching 3.3 g/L and GlcNAc titer being less than 5 g/L (Fig. 3c–e). However, the slow utilization of urea in the starting strain was not enough to counteract the acidification during fermentation, with the decrease of pH_{ex} from 7.5 to 5.9 and the pH_{in} to 6.0, and so could not alleviate the inhibition of pyruvate on the key enzyme CeGNA1 (Fig. 3c).

The above results demonstrated that the expression level of urease should be neither too high nor too low. Because a decrease in pH_{in} and pH_{ex} mainly occurred at the early phase of fermentation, the expression of urease should correspond to this phase to alleviate the decrease of pH_{in} and pH_{ex} , and then it should be low enough to avoid excessive alkalization during fermentation. To achieve this, two classes of phase-dependent auto-inducible promoters, exponential phase-dependent promoters (P_{abrB} and P_{hag} , with P_{abrB} being stronger than P_{hag}) and middle-log phase-dependent promoters (P_{ffh} and P_{licH} , with P_{ffh} being stronger than P_{licH}), were chosen to control the expression of urease (Fig. 4a) [17].

As shown in Fig. 4, urea utilization depended on the strength and class of the chosen promoters. Consistent with what was described above, strong promoters (P_{abrB} and P_{ffh}), which resulted in rapid utilization of urea and excessive alkalization during fermentation, were not suitable for urease expression and GlcNAc production here. In comparison, the weak promoters (P_{hag} and P_{licH}) were more suitable for urease expression and GlcNAc production, especially the exponential phase-dependent promoter P_{hag} . Promoter P_{hag} promoted the slow utilization of urea, which was consumed within 36 h, and alleviated the decrease of pH_{in} , with the lowest pH_{in} increasing from 6.0 to 6.8 (Fig. 4b, c). Meanwhile, the lowest pH_{ex} also increased from 5.9 to 6.4. As a result, the cells grew better, with the maximum DCW 9.0 g/L being 15.2% higher than that of the starting strain BSGN12 at 24 h, and the GlcNAc titer and yield reached 25.6 g/L and 0.43 g GlcNAc/g glucose at the end of the fermentation, which were 1.39- and 1.36-fold of that of the starting strain BSGN12, respectively (Fig. 4d, e).

Production of GlcNAc by BSGN13 in a 3-L fermenter

As shown in Fig. 5, there was no overflow of pyruvate in the broth during the fed-batch. The engineered *B. subtilis*



BSGN13 grew continuously from 0 to 36 h and reached a maximum DCW of 20.7 g/L at 36 h. The GlcNAc in the broth accumulated rapidly along with cell growth and reached 59.8 g/L at 36 h, with an average GlcNAc productivity of 1.66 g/L per hour. Though GlcNAc accumulated gradually from 36 to 56 h and reached 82.5 g/L with a yield of 0.39 g GlcNAc/g glucose, which was 1.7- and 1.2-fold of that produced before (48.9 g/L GlcNAc and 0.32 g GlcNAc/g glucose), the average GlcNAc productivity of 1.13 g/L per hour was obviously decreased [5].

The decreased GlcNAc productivity maybe due to a shortage of nitrogen supply, because even if all the urea

and $(NH_4)_2SO_4$ in the medium were converted to GlcNAc by 100%, only 56.8 g/L GlcNAc could be synthesized, which was 65% of 82.5 g/L. This indicated that most of the nitrogen in GlcNAc originate from yeast extract (12 g/L) and tryptone (6 g/L). Actually, lots of ammonia from urea was used to neutralize the pH_{in} , and much of the yeast extract and tryptone were used for cell growth. In the future, we will further study the supply and balance of nitrogen sources to promote GlcNAc production.

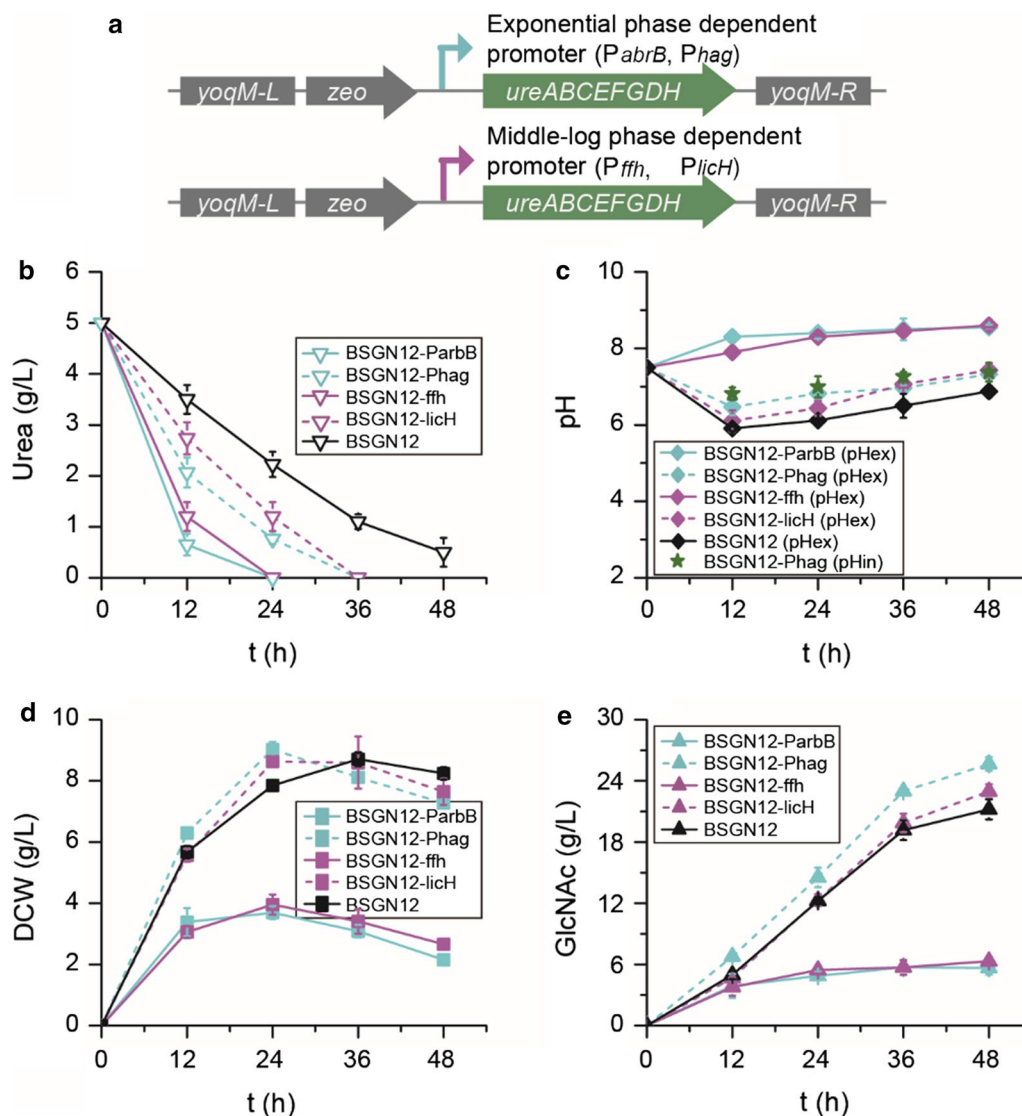


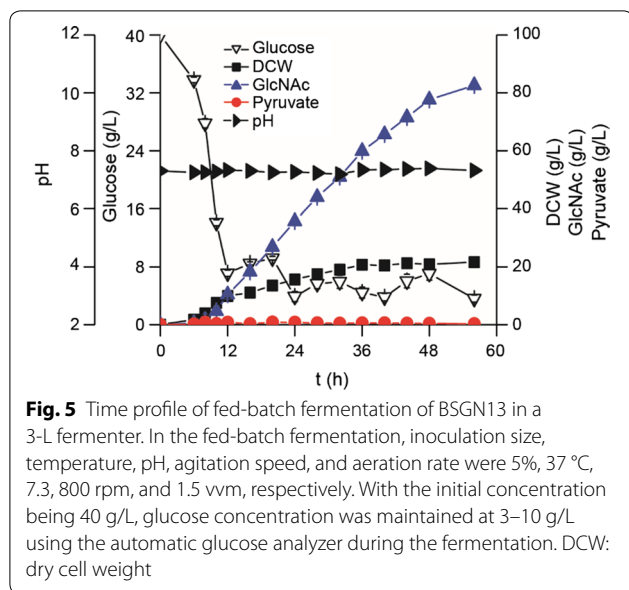
Fig. 4 Effects of urease expression on GlcNAc fermentation. **a** Expression of urease were controlled by the exponential phase dependent promoters (P_{abrB} and P_{hag}) and middle-log phase dependent promoters (P_{ffh} and P_{licH}), respectively. Effects of urease expression on urea utilization (**b**), pH (**c**), cell growth (dry cell weight, DCW) (**d**) and GlcNAc production (**e**)

Discussion

It is well known that pyruvate is synthesized from Fru-6P through Embden–Meyerhof–Parnas pathway, and further converted to Ac-CoA. Since synthesis of GlcNAc consumes Fru-6P and Ac-CoA, which competes with pyruvate synthesis and promoting pyruvate utilization, it was speculated that the overflow of pyruvate indicated the synthesis pathway of GlcNAc was not strong enough to divert carbon flux from pyruvate. To enhance the synthesis pathway of GlcNAc and promote GlcNAc production, the two key enzymes *CeGNA1* and glucosamine-6-phosphate synthase (*GlmS*) were previously

overexpressed, which decreased pyruvate concentration significantly [6]. However, the residual pyruvate dropped the pH_{in} , inhibiting the *CeGNA1* activity. Hence, for alleviating pyruvate burden and enhancing GlcNAc production in this study, the key enzyme *CeGNA1* was further modified to increase its catalytic efficiency.

A lot of effort has been made to engineer pathway enzymes in metabolic engineering for improved production of value-added biological chemicals [22–24]. Among them, Ep-PCR based directed evolution is a powerful strategy for adapting enzyme properties to specific needs. In the study, Ep-PCR mutation of the *cegnal* gene



conferred it enhanced acid-resistance. Because the wild-type *CeGNA1* has a pH optimum in the alkaline range (8.2), its activity under acid conditions was low, so we looked for acid resistant forms of the enzyme to improve the yield of GlcNAc. Indeed, owing to limited catalytic performance, the enzymes harvested from nature's biodiversity often need to be improved for their desired functions. This study also highlighted the importance of pathway protein engineering to efficiently produce value-added biological chemicals in microbial factories.

Although mutations of the key enzyme *CeGNA1* improved its catalytic efficiency during pyruvate stress and promoted GlcNAc production in this study, during this process, we found that the commonly used plasmid-based expression systems were prone to genetic instability. For high-level, genetically stable expression of the key enzyme *CeGNA1*, it is interesting to construct a plasmid-free, high gene copy expression system for GlcNAc production in the future. Maybe integration of *CeGNA1* into the genome and regulation of the ratio of *CeGNA1* to *GlmS*, two key enzymes catalyzing two consecutive reactions within GlcNAc synthesis pathway, using artificial protein scaffolds are beneficial for *CeGNA1* expression and enhanced metabolic flux channeling to promote GlcNAc production [1, 25].

It has been reported that urease, which catalyzes the hydrolysis of urea to two molecules of ammonia and one molecule of carbon dioxide, plays important roles in maintaining pH_{in} homeostasis and providing ammonium for nitrogen metabolism, which are widely used in metabolic engineering and synthetic biotechnology [26, 27]. Though *B. subtilis* contains urease structural genes,

it lacks the accessory genes typically required for GTP-dependent incorporation of nickel, which is essential for urease maturation [28, 29]. For those reasons, urease from *B. paralicheniformis* was heterologously expressed here [16]. Consistent with previous reports where the urease overexpressing *Saccharomyces cerevisiae* strain grew 30–50% slower than the control strain, the strong promoter-controlled expression of urease herein remarkably inhibited BSGN12 growth [27]. However, Milne et al. [27] reported that the cell growth decrease was probably due to ammonia release due to the overexpression of urease, which alkalized the pH_{in} and pH_{ex} . Of course, there might have been other factors that also contributed to the cell growth decrease.

Conclusions

Here, we described mutations of the key enzyme *CeGNA1* and heterologous expression of urease from *B. paralicheniformis* to counteract the pyruvate stress for GlcNAc production. The Q155V/C158G mutations enhanced the activity of *CeGNA1* by 11.5% and increased the catalytic efficiency by 27.5%, making *CeGNA1*-Q155V/C158G a promising candidate for GlcNAc production, with the GlcNAc titer increasing to 20.9 g/L in shake flask fermentation. Urease expression under the control of the exponential phase-dependent promoter P_{hag} increased pH_{in} from 6.0 to 6.8, relieved acid stress on key enzyme *CeGNA1*, and increased the titer and yield of GlcNAc to 25.6 g/L and 0.43 g GlcNAc/g glucose, respectively. Finally, in a 3-L fermenter, there was no pyruvate overflow, and the GlcNAc titer reached 82.5 g/L, which was 1.7-fold of that produced before. It was recognized that the pathway enzyme engineering and host engineering regarding urea metabolism were of particular importance to overcome pyruvate overflow for achieving high biosynthesis efficiency of GlcNAc.

Additional file

Additional file 1: Table S1. Primers used in this study. **Fig S1.** The mutagenesis selection process. **Fig S2.** Comparison of the activities of strains with single Q155V and C158G mutants and saturation mutagenesis of C158. **Fig S3.** Identify the double band around 38–39 KDa on the SDS-PAGE.

Abbreviations

GNA1: glucosamine-6-phosphate *N*-acetyltransferase; GlcNAc: *N*-acetylglucosamine; *B. subtilis*: *Bacillus subtilis*; *CeGNA1*: GNA1 from *Caenorhabditis elegans*; pH_{in} : intracellular pH; Ep-PCR: error prone PCR; GlcNAc-6P: GlcNAc-6-phosphate; GlcN-6P: glucosamine-6-phosphate.

Authors' contributions

WLM, YFL and LL designed the study. WLM performed the experiments and analyzed the data. WLM and XQL wrote the manuscript with contributions from all authors. WLM and LL reviewed and edited the manuscript. All authors read and approved the final manuscript.

Author details

¹ Key Laboratory of Carbohydrate Chemistry and Biotechnology, Ministry of Education, Jiangnan University, Wuxi 214122, China. ² Key Laboratory of Industrial Biotechnology, Ministry of Education, Jiangnan University, Wuxi 214122, China.

Acknowledgements

Not applicable.

Competing interests

The authors declare that they have no competing interests.

Availability of data and materials

All data generated or analyzed during this study are included in this published article and the Additional file 1.

Consent for publication

Not applicable.

Ethics approval and consent to participate

Not applicable.

Funding

This work was financially supported by the National Natural Science Foundation of China (31622001, 31671845, 21676119, 31600068), the Natural Science Foundation of Jiangsu Province (BK20160176), "the Fundamental Research Funds for the Central Universities"-China (JUSRP11725), the 111 Project-China (No. 111-2-06), and the China Postdoctoral Science Foundation (2016M600363, 2017T100327, 2018M630523).

Publisher's Note

Springer Nature remains neutral with regard to jurisdictional claims in published maps and institutional affiliations.

Received: 9 September 2018 Accepted: 24 December 2018

Published online: 04 January 2019

References

- Liu YF, Zhu YQ, Ma WL, Shin HD, Li JH, Liu L, Du GC, Chen J. Spatial modulation of key pathway enzymes by DNA-guided scaffold system and respiration chain engineering for improved *N*-acetylglucosamine production by *Bacillus subtilis*. *Metab Eng*. 2014;24:61–9.
- Longo DL, Moustaghfir FZ, Zerbo A, Consolino L, Anemone A, Bracesco M, Aime S. EXCI-CEST: exploiting pharmaceutical excipients as MRI-CEST contrast agents for tumor imaging. *Int J Pharm*. 2017;525:275–81.
- Ud-Din A, Tikhomirova A, Roujeinikova A. Structure and functional diversity of GCN5-related *N*-acetyltransferases (GNAT). *Int J Mol Sci*. 2016;17:45.
- Dorfmueller HC, Fang W, Rao FV, Blair DE, Attrill H, van Aalten DM. Structural and biochemical characterization of a trapped coenzyme A adduct of *Caenorhabditis elegans* glucosamine-6-phosphate *N*-acetyltransferase 1. *Acta Crystallogr D Biol Crystallogr*. 2012;68:1019–29.
- Ma W, Liu Y, Shin H, Li J, Chen J, Du G, Liu L. Metabolic engineering of carbon overflow metabolism of *Bacillus subtilis* for improved *N*-acetylglucosamine production. *Bioresour Technol*. 2018;250:642–9.
- Ma W, Liu Y, Wang Y, Lv X, Li J, Du G, Liu L. Combinatorial fine-tuning of GNA1 and GlnS expression by 5'-terminus fusion engineering leads to overproduction of *N*-acetylglucosamine in *Bacillus subtilis*. *Biotechnol J*. 2018. <https://doi.org/10.1002/biot.201800264>.
- Pandey R, Vischer NOE, Smelt J, van Beilen JWA, Ter Beek A, De Vos WH, Brul S, Manders EMM. Intracellular pH response to weak acid stress in individual vegetative *Bacillus subtilis* cells. *Appl Environ Microbiol*. 2016;82:6463–71.
- Pham HL, Wong A, Chua N, Teo WS, Yew WS, Chang MW. Engineering a riboswitch-based genetic platform for the self-directed evolution of acid-tolerant phenotypes. *Nat Commun*. 2017;8:411.
- van Beilen JWA, Brul S. Compartment-specific pH monitoring in *Bacillus subtilis* using fluorescent sensor proteins: a tool to analyze the antibacterial effect of weak organic acids. *Front Microbiol*. 2013;4:11.
- Guo SQ, Zhang SJ, Fang XL, Liu Q, Gao JT, Bilal M, Wang YH, Zhang X. Regulation of antimicrobial activity and xenocoumarins biosynthesis by pH in *Xenorhabdus nematophila*. *Microb Cell Fact*. 2017;16:14.
- Feng SS, Yang HL, Wang W. System-level understanding of the potential acid-tolerance components of *Acidithiobacillus thiooxidans* ZJJN-3 under extreme acid stress. *Extremophiles*. 2015;19:1029–39.
- Asteriou T, Deschrevel B, Delpech B, Bertrand P, Bultelle F, Merai C, Vincent JC. An improved assay for the *N*-acetyl- β -glucosamine reducing ends of polysaccharides in the presence of proteins. *Anal Biochem*. 2001;293:53–9.
- Liu H, Naismith JH. An efficient one-step site-directed deletion, insertion, single and multiple-site plasmid mutagenesis protocol. *BMC Biotechnol*. 2008;8:91.
- Yang HQ, Lu XY, Liu L, Li JH, Shin HD, Chen RR, Du GC, Chen J. Fusion of an oligopeptide to the N terminus of an alkaline alpha-amylase from *Alkalimonas amyolytica* simultaneously improves the enzyme's catalytic efficiency, thermal stability, and resistance to oxidation. *Appl Environ Microbiol*. 2013;79:3049–58.
- Zhu BY, Stulke J. SubtiWiki in 2018: from genes and proteins to functional network annotation of the model organism *Bacillus subtilis*. *Nucleic Acids Res*. 2018;46:D743–8.
- Liu QT, Chen YQ, Yuan ML, Du GC, Chen J, Kang Z. A *Bacillus paralicheniformis* iron-containing urease reduces urea concentrations in rice wine. *Appl Environ Microbiol*. 2017;83:11.
- Yang S, Du GC, Chen J, Kang Z. Characterization and application of endogenous phase-dependent promoters in *Bacillus subtilis*. *Appl Microbiol Biotechnol*. 2017;101:4151–61.
- Shevchuk NA, Bryksin AV, Nusinovich YA, Cabello FC, Sutherland M, Ladisch S. Construction of long DNA molecules using long PCR-based fusion of several fragments simultaneously. *Nucleic Acids Res*. 2004;32:e19.
- Yan X, Yu HJ, Hong Q, Li SP. Cre/lox system and PCR-based genome engineering in *Bacillus subtilis*. *Appl Environ Microbiol*. 2008;74:5556–62.
- Clark S, Francis PS, Conlan XA, Barnett NW. Determination of urea using high-performance liquid chromatography with fluorescence detection after automated derivatisation with xanthidrol. *J Chromatogr*. 2007;1161:207–13.
- Liu YF, Liu L, Shin HD, Chen RR, Li JH, Du GC, Chen J. Pathway engineering of *Bacillus subtilis* for microbial production of *N*-acetylglucosamine. *Metab Eng*. 2013;19:107–15.
- Li R, Wijma HJ, Song L, Cui Y, Otzen M, Tian Ye DuJ, Li T, Niu D, Chen Y, Feng J, Han J, Chen H, Tao Y, Janssen DB, Wu B. Computational redesign of enzymes for regio- and enantioselective hydroamination. *Nat Chem Biol*. 2018;14:664.
- Dumas L, Zito F, Auroy P, Johnson X, Peltier G, Alric J. Structure-function analysis of chloroplast proteins via random mutagenesis using error-prone PCR. *Plant Physiol*. 2018;177:465–75.
- Liu XL, Liang MJ, Liu YH, Fan XJ. Directed evolution and secretory expression of a pyrethroid-hydrolyzing esterase with enhanced catalytic activity and thermostability. *Microb Cell Fact*. 2017;16:12.
- Chen XL, Zhu P, Liu LM. Modular optimization of multi-gene pathways for fumarate production. *Metab Eng*. 2016;33:76–85.
- Shaw AJ, Covalla SF, Miller BB, Firliet BT, Hogsett DA, Herring CD. Urease expression in a *Thermoanaerobacterium saccharolyticum* ethanologen allows high titer ethanol production. *Metab Eng*. 2012;14:528–32.
- Milne N, Luttik MAH, Rojas HFC, Wahl A, van Maris AJA, Pronk JT, Daran JM. Functional expression of a heterologous nickel-dependent, ATP-independent urease in *Saccharomyces cerevisiae*. *Metab Eng*. 2015;30:130–40.
- Mols M, Abee T. Role of ureolytic activity in *Bacillus cereus* nitrogen metabolism and acid survival. *Appl Environ Microbiol*. 2008;74:2370–8.

29. Kim JK, Mulrooney SB, Hausinger RP. Biosynthesis of active *Bacillus subtilis* urease in the absence of known urease accessory proteins. *J Bacteriol.* 2005;187:7150–4.
30. Liu YF, Zhu YQ, Li JH, Shin HD, Chen RR, Du GC, Liu L, Chen J. Modular pathway engineering of *Bacillus subtilis* for improved *N*-acetylglucosamine production. *Metab Eng.* 2014;23:42–52.
31. Biedendieck R, Yang Y, Deckwer WD, Malten M, Jahn D. Plasmid system for the intracellular production and purification of affinity-tagged proteins in *Bacillus megaterium*. *Biotechnol Bioeng.* 2007;96:525–37.

Ready to submit your research? Choose BMC and benefit from:

- fast, convenient online submission
- thorough peer review by experienced researchers in your field
- rapid publication on acceptance
- support for research data, including large and complex data types
- gold Open Access which fosters wider collaboration and increased citations
- maximum visibility for your research: over 100M website views per year

At BMC, research is always in progress.

Learn more biomedcentral.com/submissions

